

United Nations/Mongolia Workshop on the Applications of Global Navigation
Satellite Systems

IONOSPHERE TEC ANOMALIES OVER MONGOLIA AS DETECTED BY GPS OBSERVATIONS

Sh. Amarjargal, D. Baatarkhuu

Astronomical Observatory of Institute of Astronomy and Geophysics, MAS

ULAANBAATAR, MONGOLIA, 25-29 OCTOBER 2021

OUTLINE

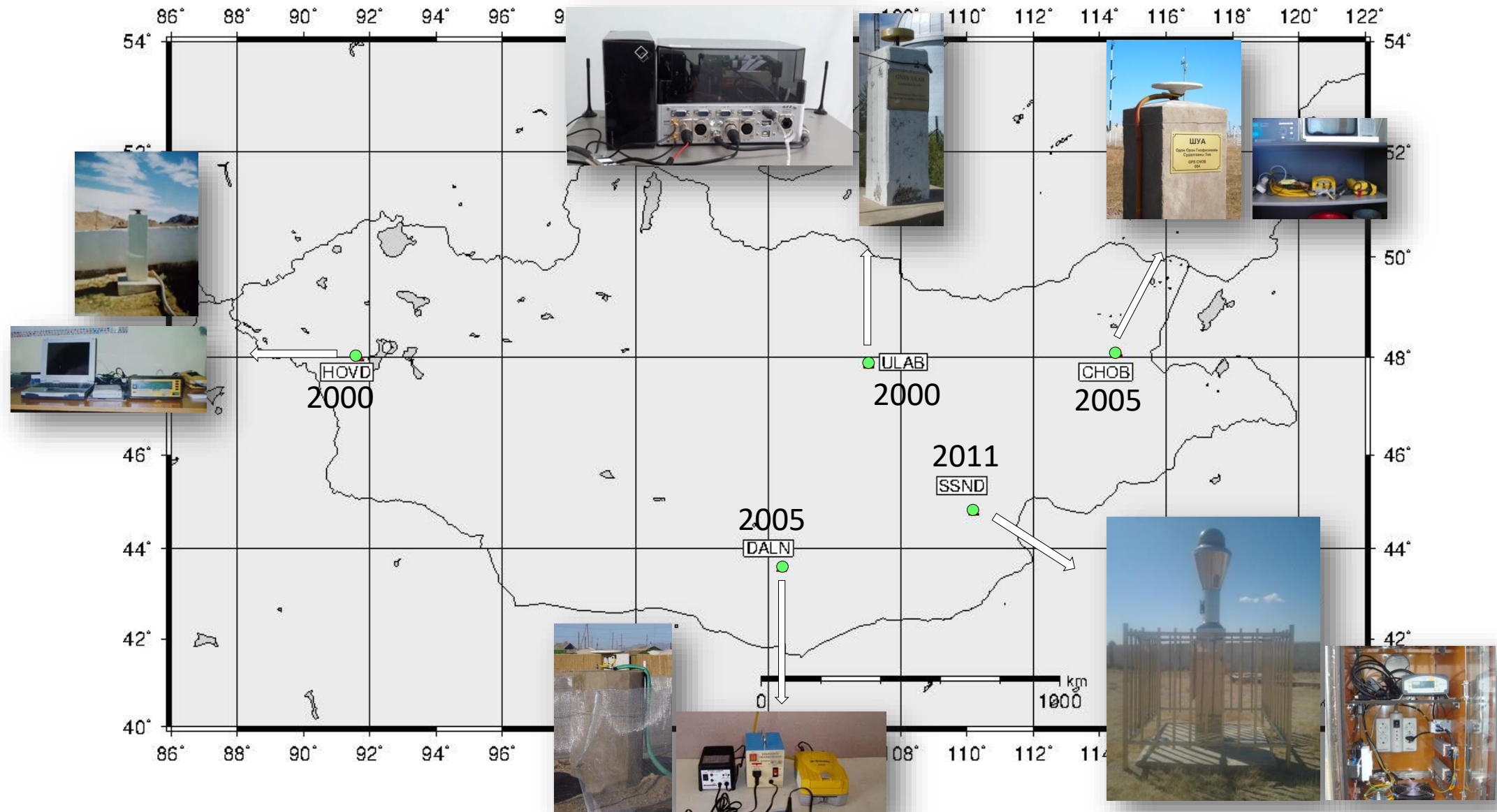
- Introduction
- Ionosphere effects on GPS geodetic measurements – noise to information
- General variability of the ionosphere TEC over Mongolia (2008-2019 TEC data CGPS stations)
 - Variations and Anomalies
 - Seasonal, semiannual and annual
 - Storm-induced
 - Seismic
- Summary

Astronomical Observatory of Mongolia

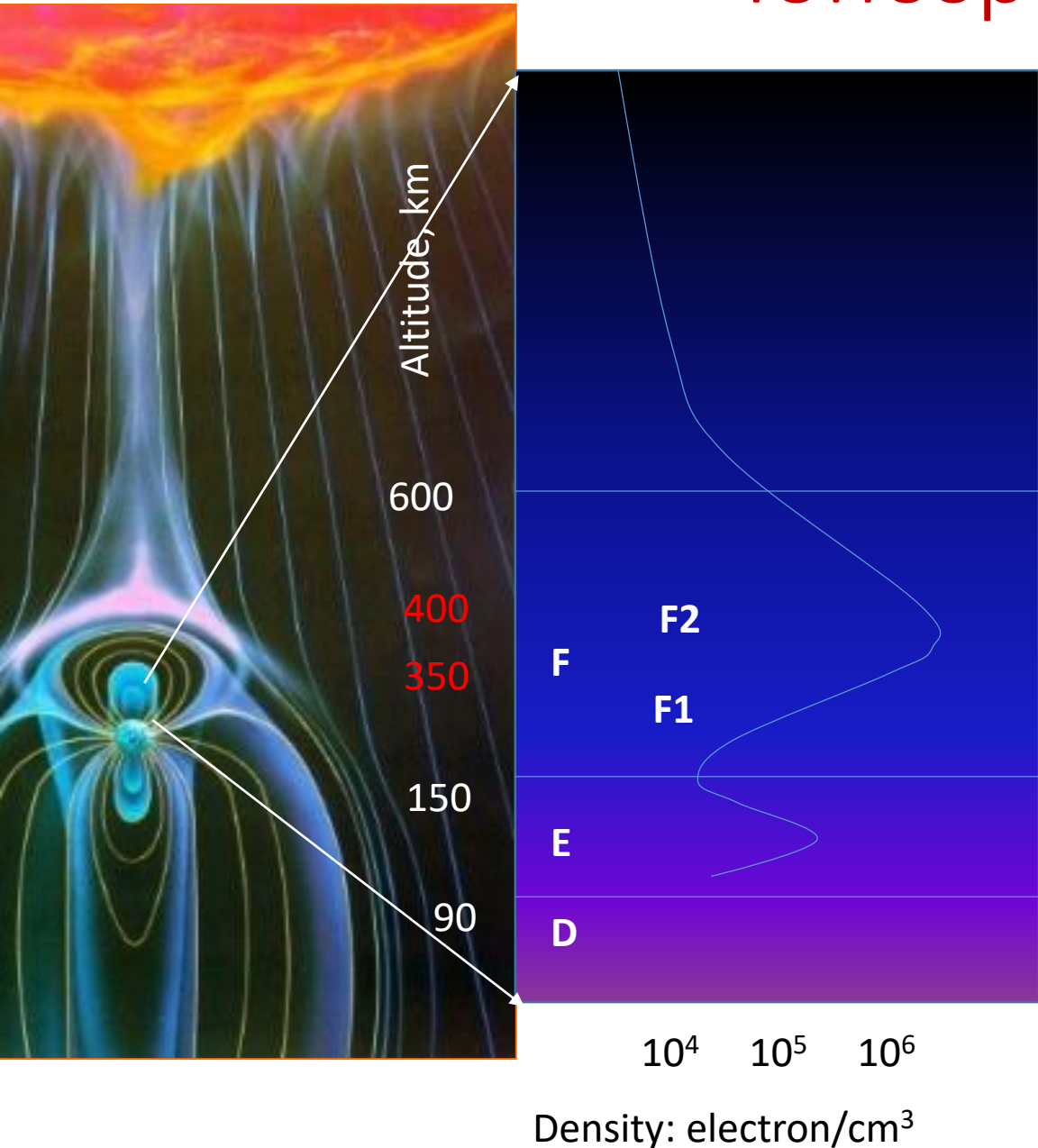


Solar flares, Sun prominences, corona, Solar burst, Solar ultra-violet radiation with radiometer, Ionosphere Total Electron Content

GPS stations of the Astronomical Observatory (AO)

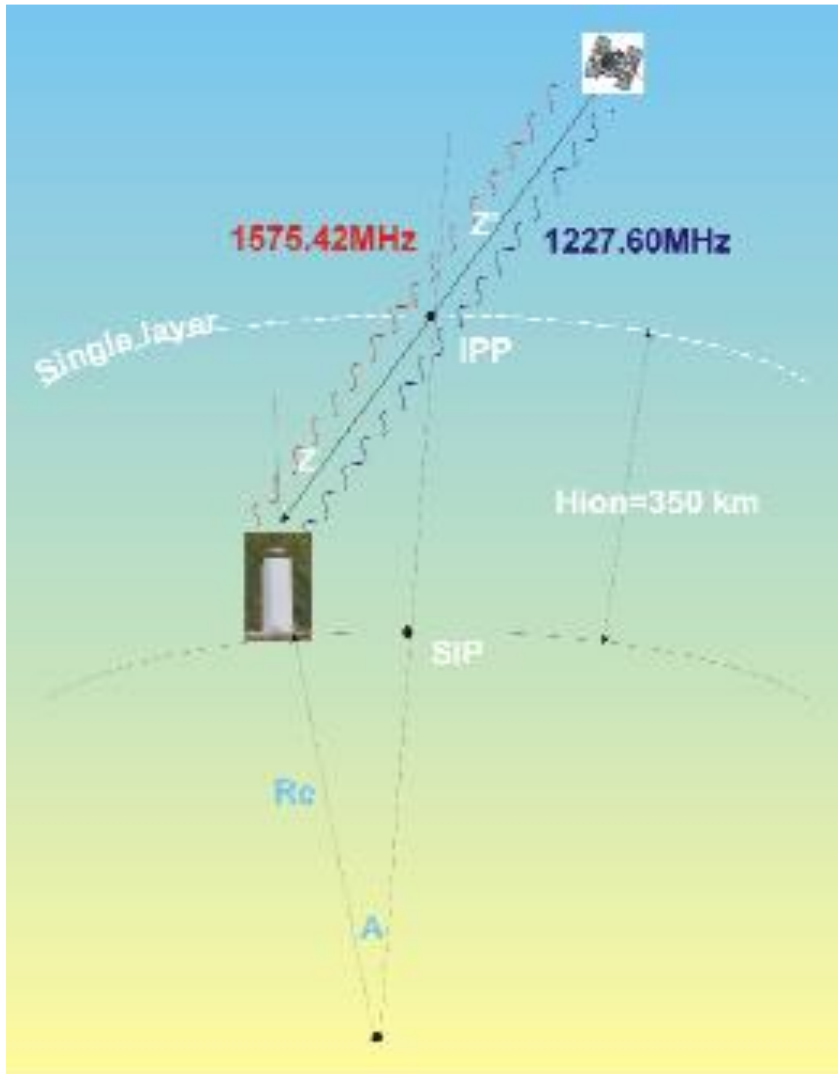


Ionosphere and the Sun



- Ionosphere is the **ionized plasma layer** of the upper atmosphere surrounding the Earth at ~60-1000 km
- The main density: 350-400 km (F2 layer)
- The main cause of the ionization – Sun EUV radiation and X-ray
- Spatial and temporal variation (geographical location, season, solar cycle and geomagnetic activity)
- Dispersive nature $1\text{Hz} < \text{signal travel}$ dependent of frequency

Ionosphere and GNSS signal propagation



- GPS signal $f_1=1227.6$ MHz, $f_2=1575.4$ MHz
- Signal delay: low frequency – high delay (GPS L2 delay > L1)
- Delay is proportional to the density of free electrons along the ray path
- $\int_r^S N_e ds = \text{STEC}$
- N_e – electron density (electron/m²)
- S – signal travel path
 - 1 TECU delay:
 - L1 - 0.163 m, L2 - 0.267 m
 - 1TECU = 10^{16} el/m²

TEC retrieval from GPS observations

$$TEC_p = \frac{1}{40.3} \left[\frac{f_1^2 \cdot f_2^2}{f_1^2 - f_2^2} \right] (P_1 - P_2 + b^s - b^r)$$

$$TEC_\Phi = \frac{1}{40.3} \left[\frac{f_1^2 \cdot f_2^2}{f_1^2 - f_2^2} \right] (L_1 \cdot \lambda_1 - L_2 \cdot \lambda_2 + B^s - B^r)$$

$$VTEC = STEC(\cos z')$$

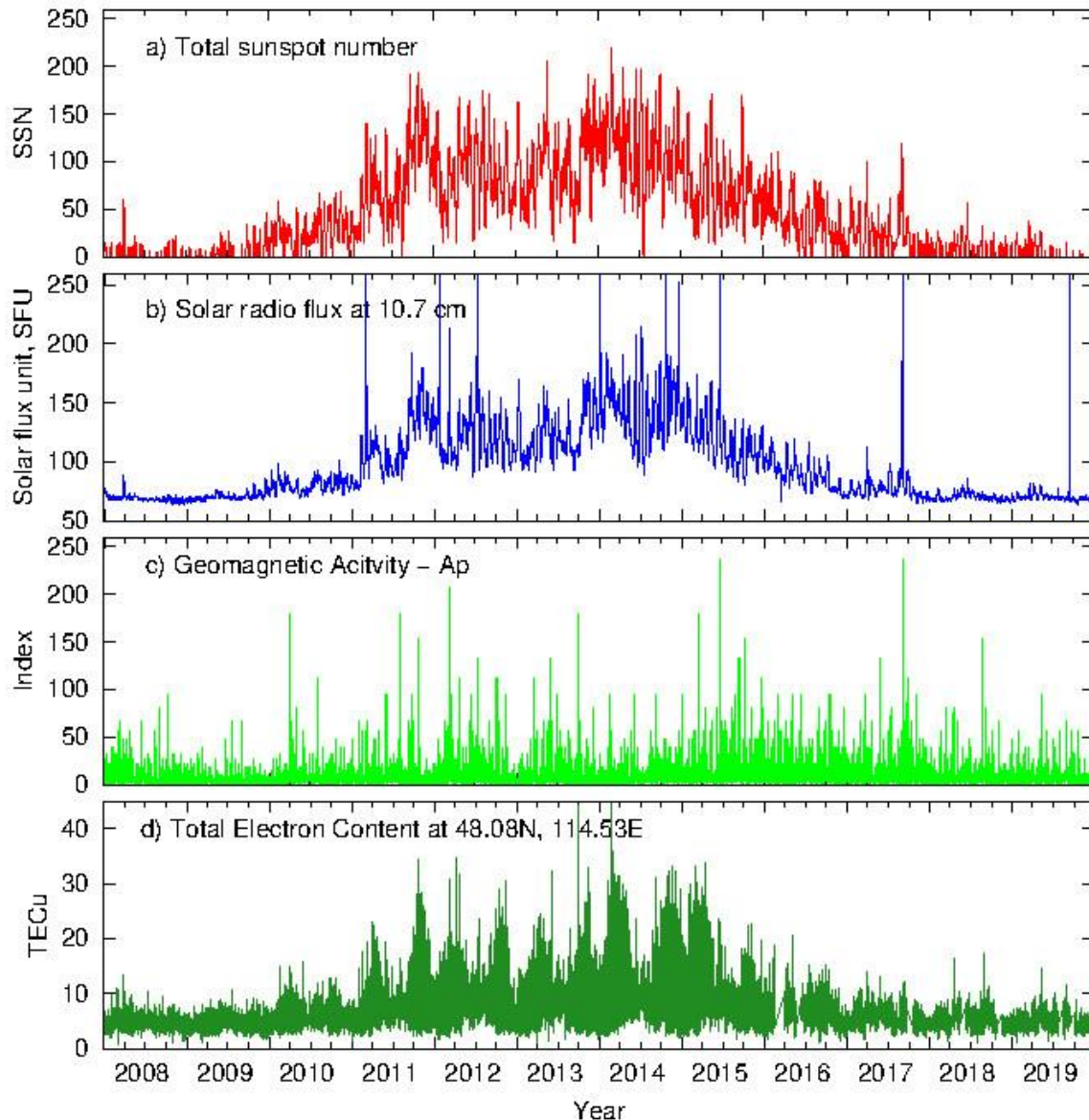
$$z' = \arcsin \left[\frac{R_e}{R_e + h_{ion}} \sin(z) \right], \quad R_e = 6371 \text{ km},$$
$$h_{ion} = 350 \text{ km}$$

- (1) calculating the difference between pseudo-ranges and carrier phases
- (2) repair cycle slips
- (3) Phase TEC leveling by pseudorange TEC
- (4) removal of the satellite and receiver biases (DCB-differential code biases);
- (5) projecting slant TEC to the vertical direction using the mapping function of the single layer model

Ionospheric variations

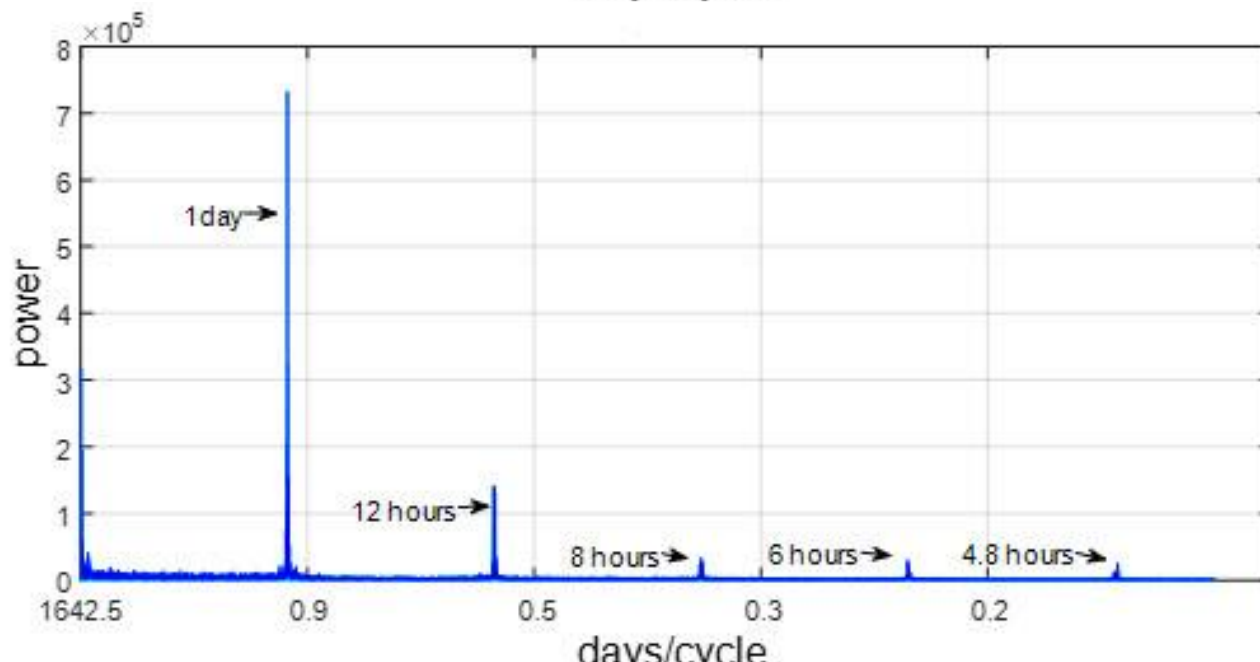
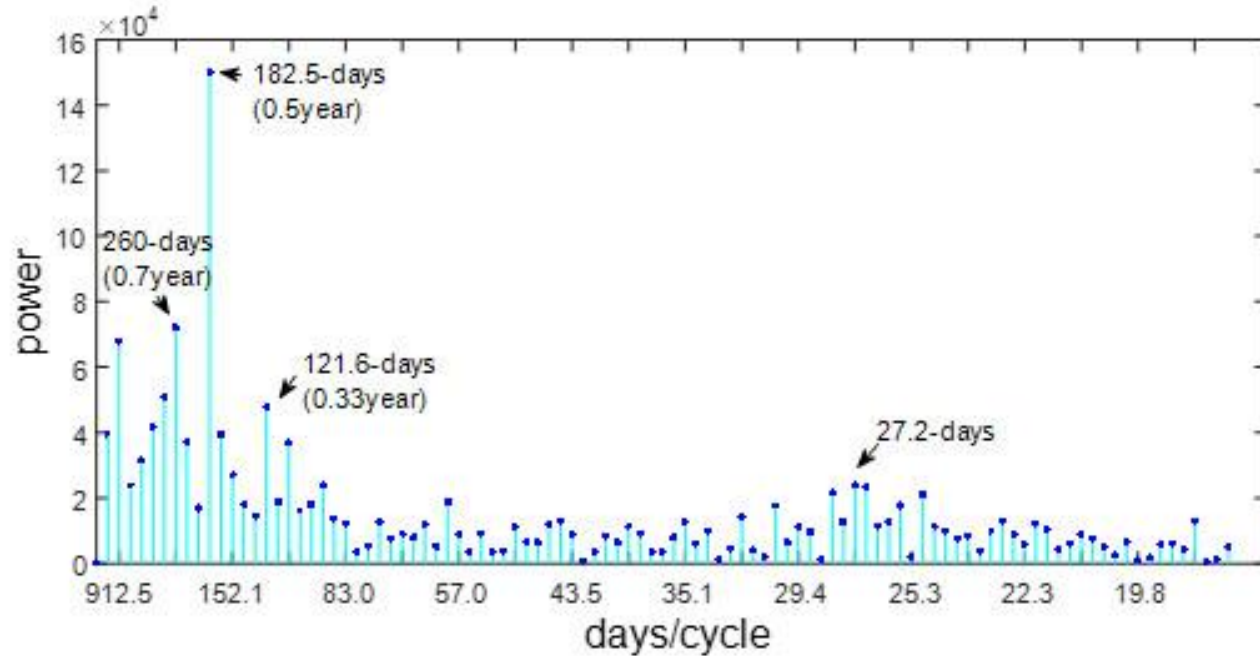
- Regular
 - diurnal, seasonal and solar cycle: *periodic -predictable*
- Irregular
 - extreme solar flare, solar wind, coronal mass ejection, geomagnetic disturbances, earthquakes and volcanic eruptions: *sudden – not predictable*
- Anomaly - Ionosphere fluctuations caused from space weather and geophysical phenomenon
- Detection (deviation from the background) – mean, median
 - Elevation cut-off angle to 40°

Mid-latitude Ionosphere variability. Solar cycle variation



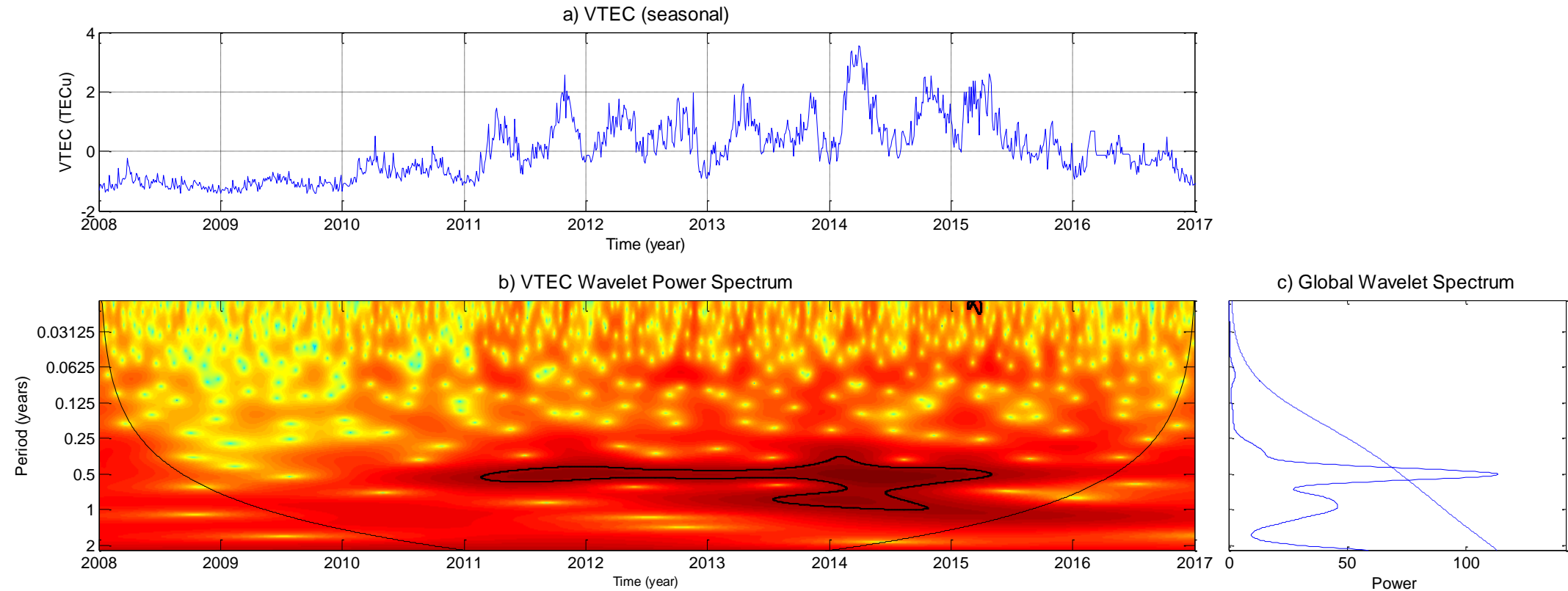
- Data on solar activity from 2008 to 2019.
- (a) Monthly mean sunspot number from WDC-SILSO, Royal Observatory of Belgium (<http://www.sidc.be/silso/datafiles>)
- (b) daily solar flux from NOAA (<http://lasp.colorado.edu/lisird/data/pentictonradioflux/>)
- (c) Geomagnetic activity indices Ap (<ftp://ftp.gfz-potsdam.de/pub/home/obs/>)
- (d) vertical TEC data from CHOB GPS station (48.08N,114.53E)

Regular variations



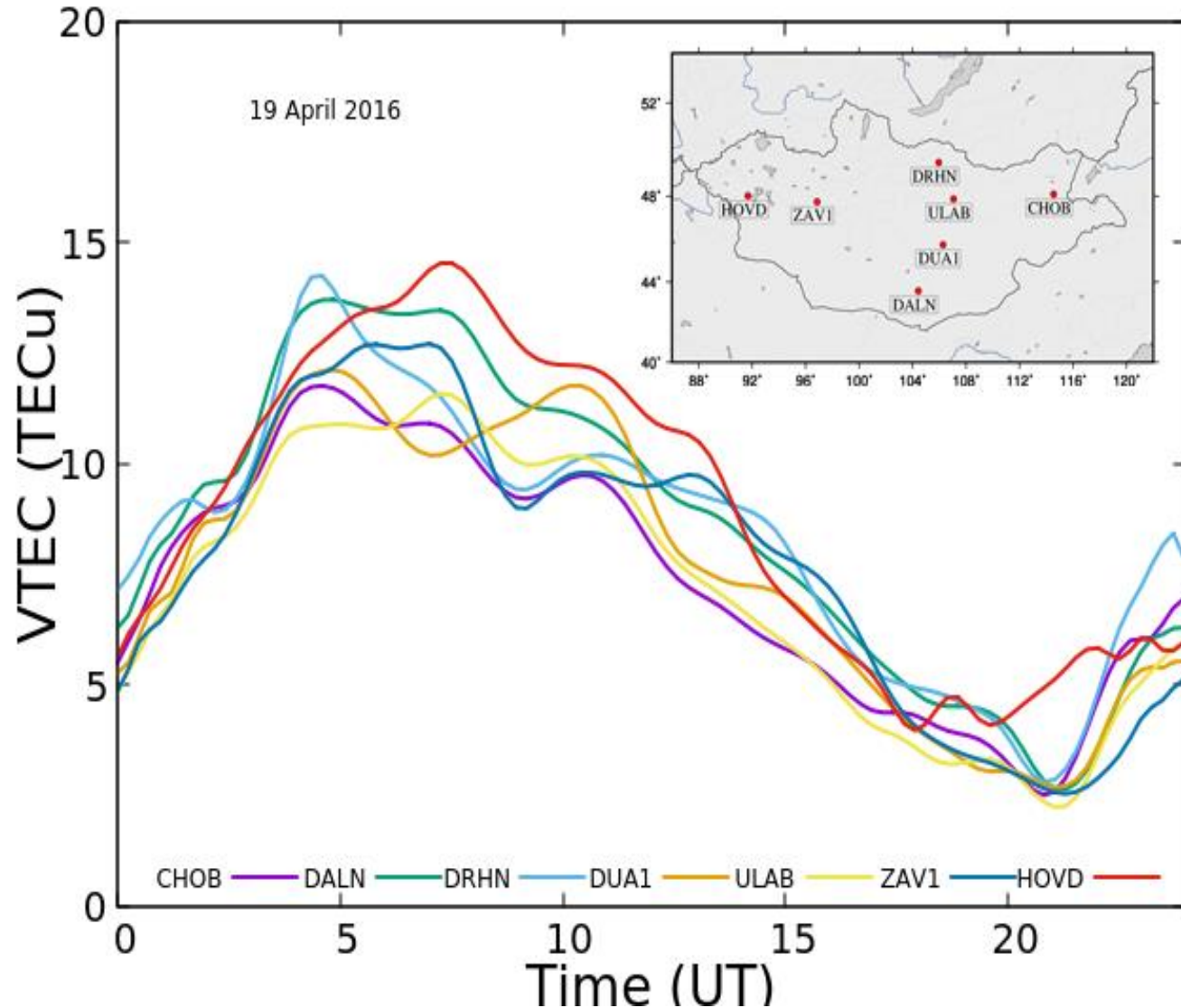
- Spectral Fourier and Wavelet analysis
- CHOB-GPS TEC 8-hour averaged data for 2008-2017
 - 260 days
 - 182.5 days
 - 121.6 days
 - 27.2 days
 - 1 day
 - 12 hours

Periodic variations (Wavelet transform)



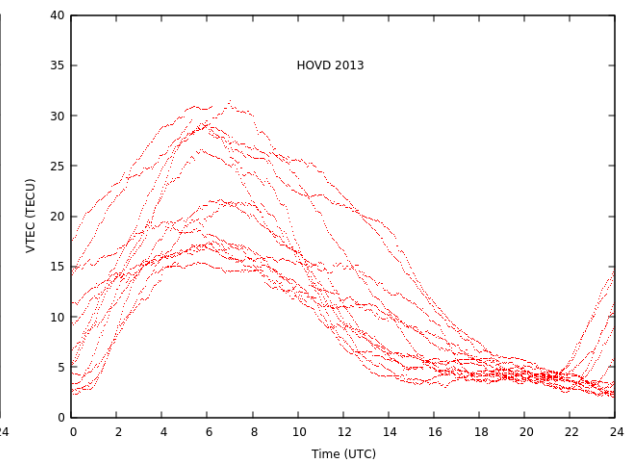
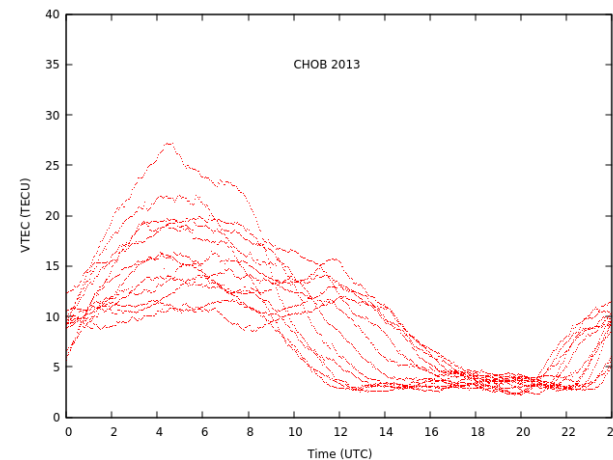
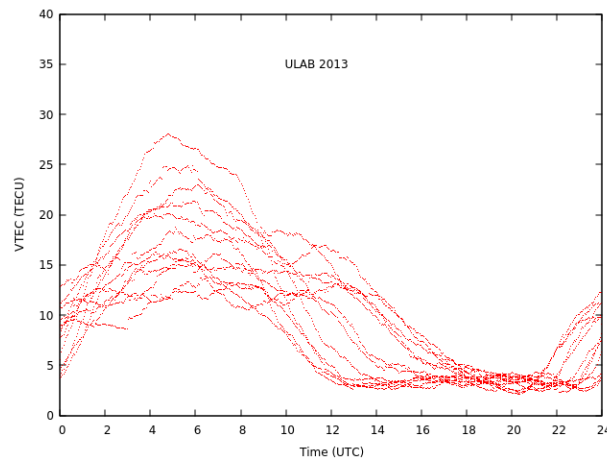
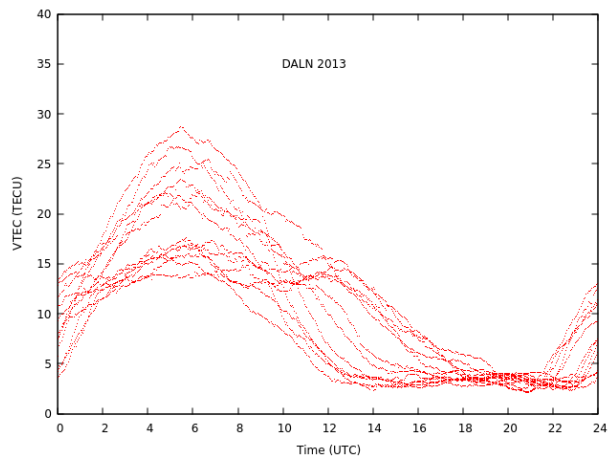
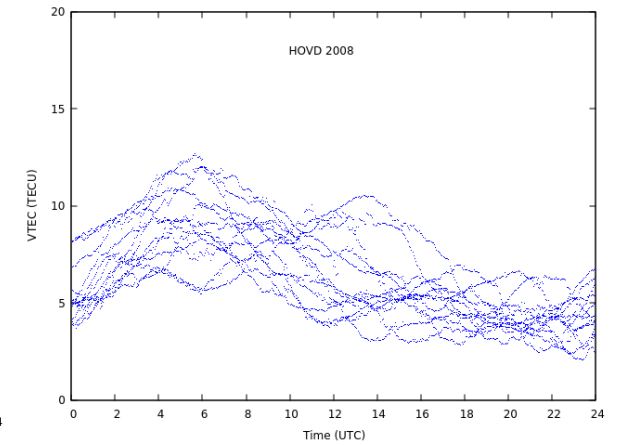
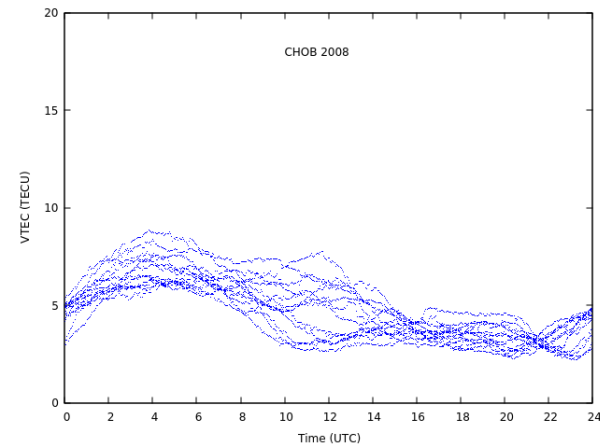
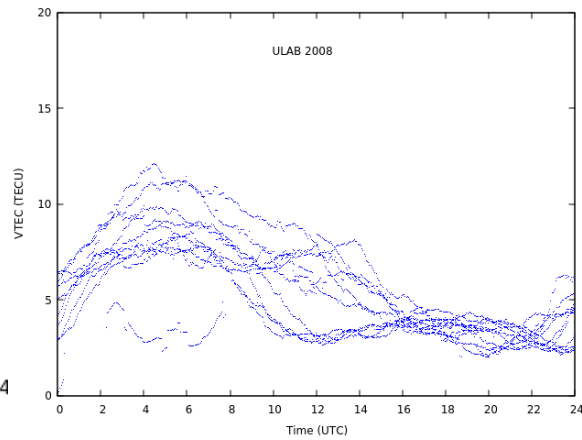
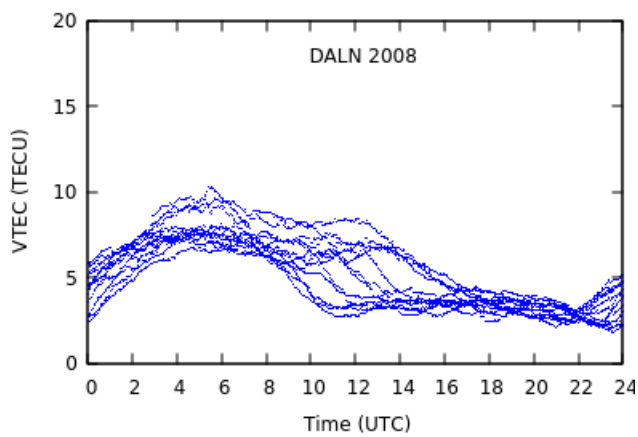
- The major significant period: semi-annual and annual cycles

Diurnal Variation



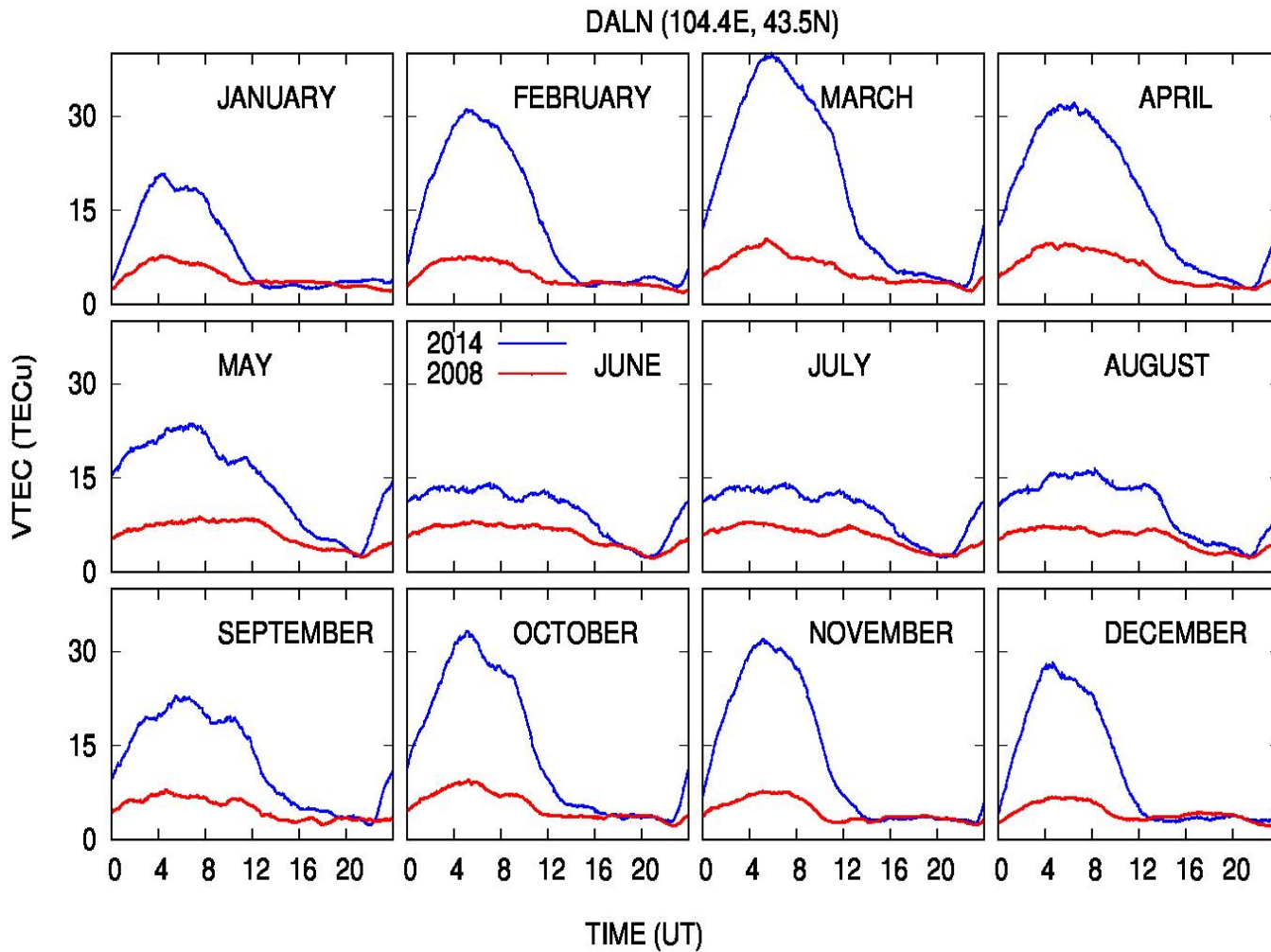
- Due to Sun movements across the sky, ionization depends on the Sun's zenith angle
- Diurnal variation from hourly mean (2016)
 - Peak at ~13LT (UTC+8h) with TEC value of 10-15 TECU
 - Kp=1 quiet condition, of descending 2016 of Solar cycle, of equinox month
 - Obvious two peaks
 - Daytime anomaly
 - Typical behavior of mid-latitude ionosphere
- Seasonal, solar activity variation

Diurnal variation



Hourly monthly median for 4 CGPS stations
During the low Solar cycle (2008) and high Solar cycle (2013) phases

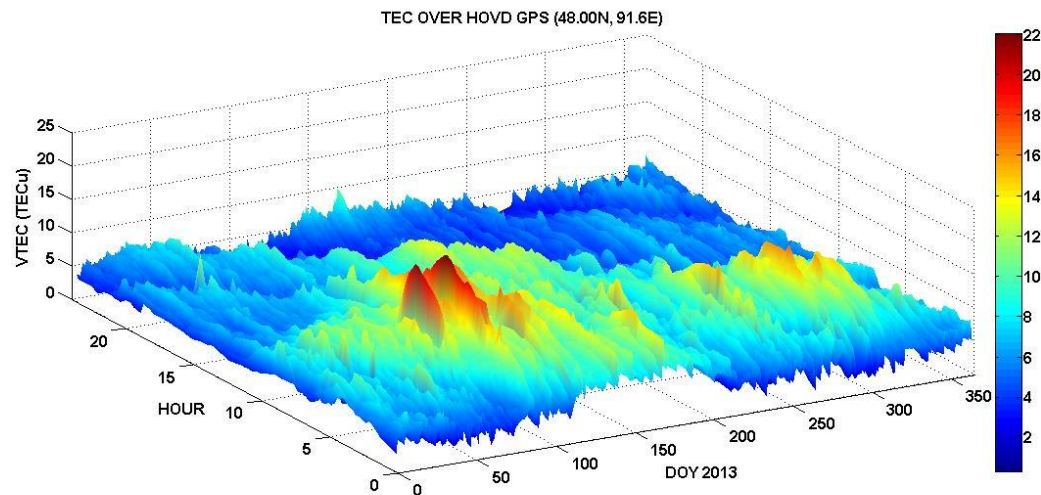
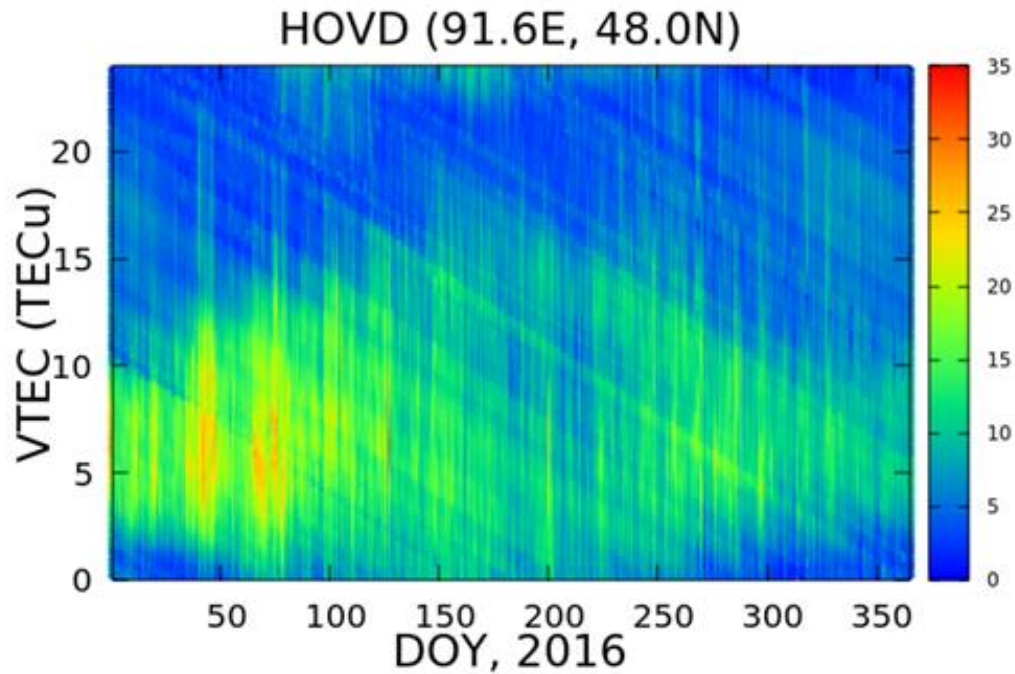
Seasonal variation



Annual or non-seasonal anomaly: December solstices are significantly greater than those in June solstices

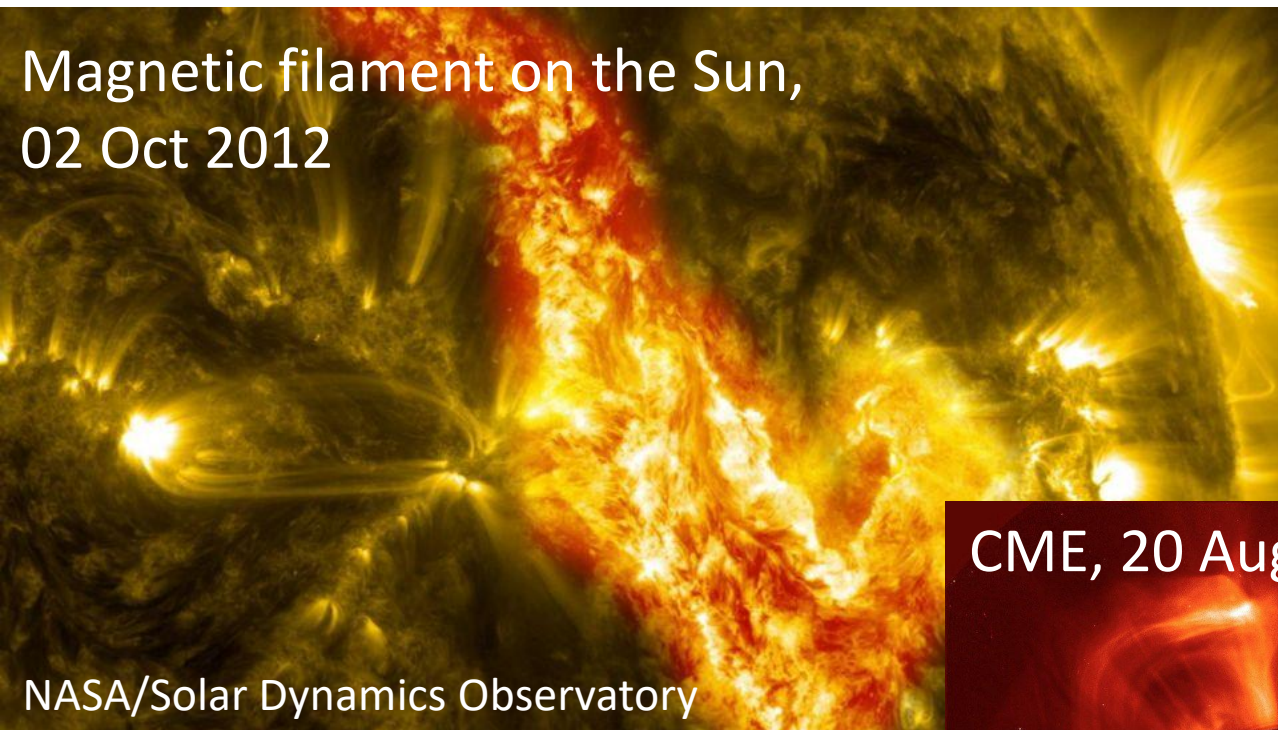
- Seasonal variation is associated with the revolution of the Earth around Sun
- Equinoctial months
 - spring-March, April, May
 - Fall-September, October, November
- Solstice months
 - Summer (June, July, August)
 - Winter (December, January, February)
- **Winter or seasonal anomaly:** ionization is greater in winter than in summer by day, but the anomaly disappears at night, NmF2 being greater in summer than in winter.

Semiannual variation



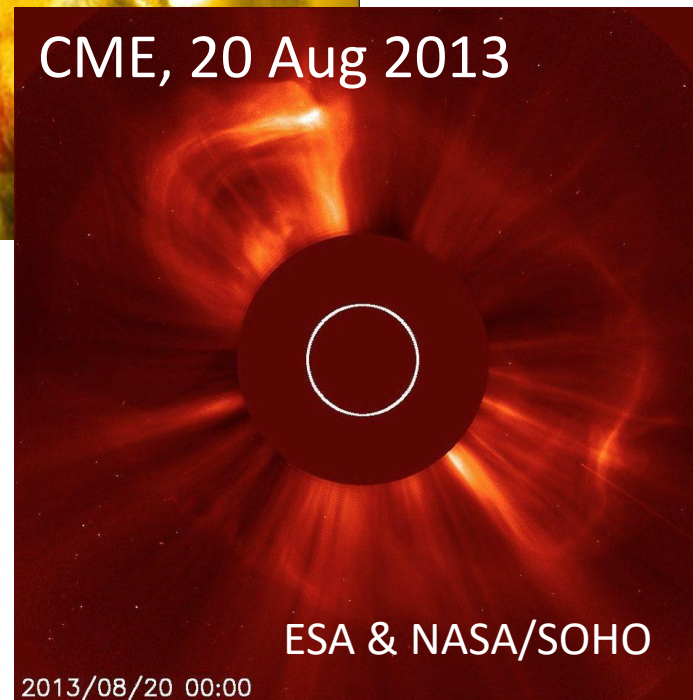
- Ionization maxima in equinoxes and minima in solstices
- **Semiannual anomaly:** ionization is greater at equinox than at solstice
- the ionization among the two equinoxes exhibits higher plasma densities in March equinox than in September equinox solstice

Solar active phenomenon

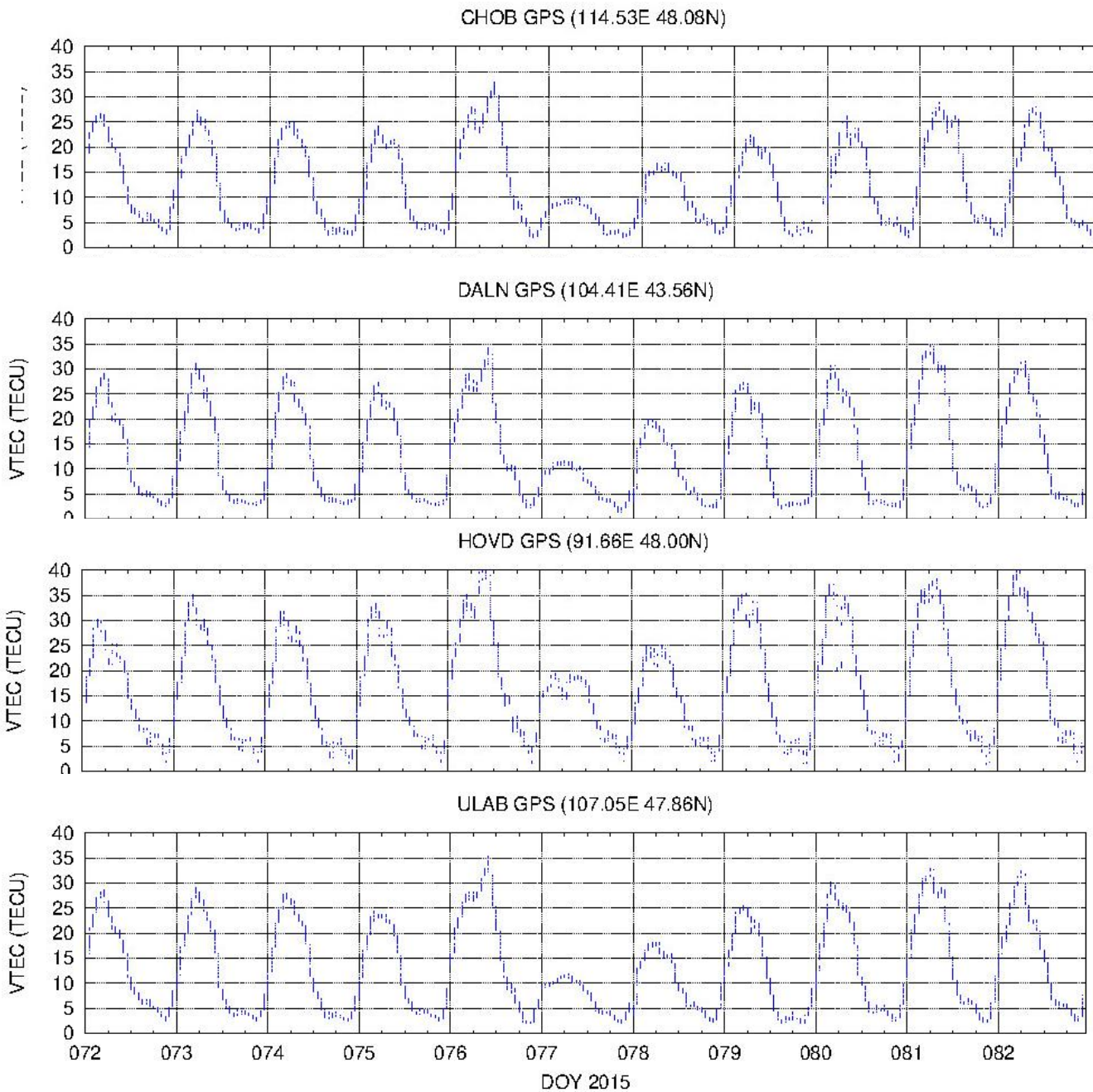


- Coronal mass ejection (CME)
- Solar flare
- Solar burst

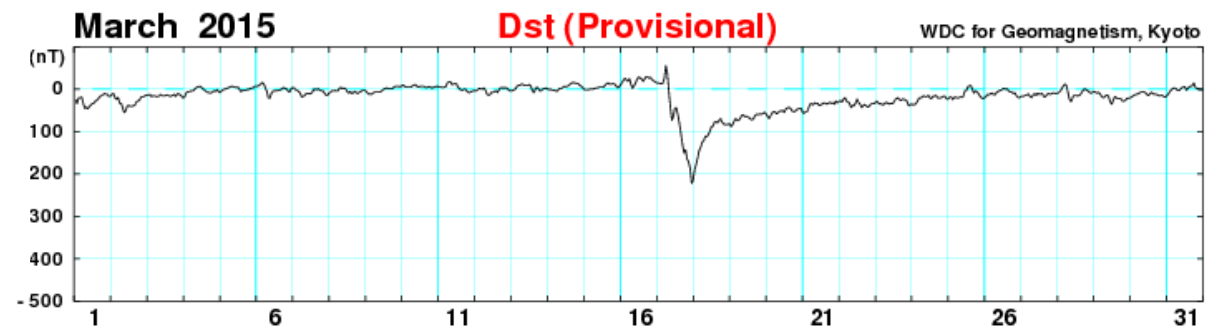
Flare activity class
X



Storm-induced anomaly (17 March 2015)

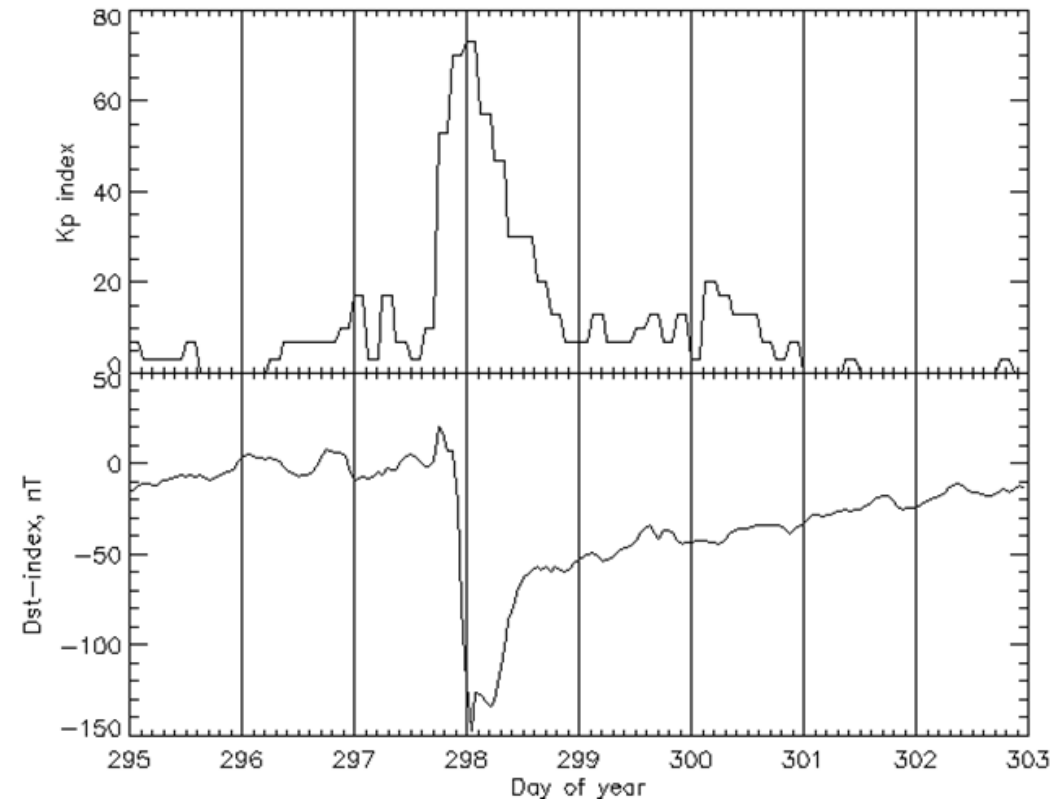
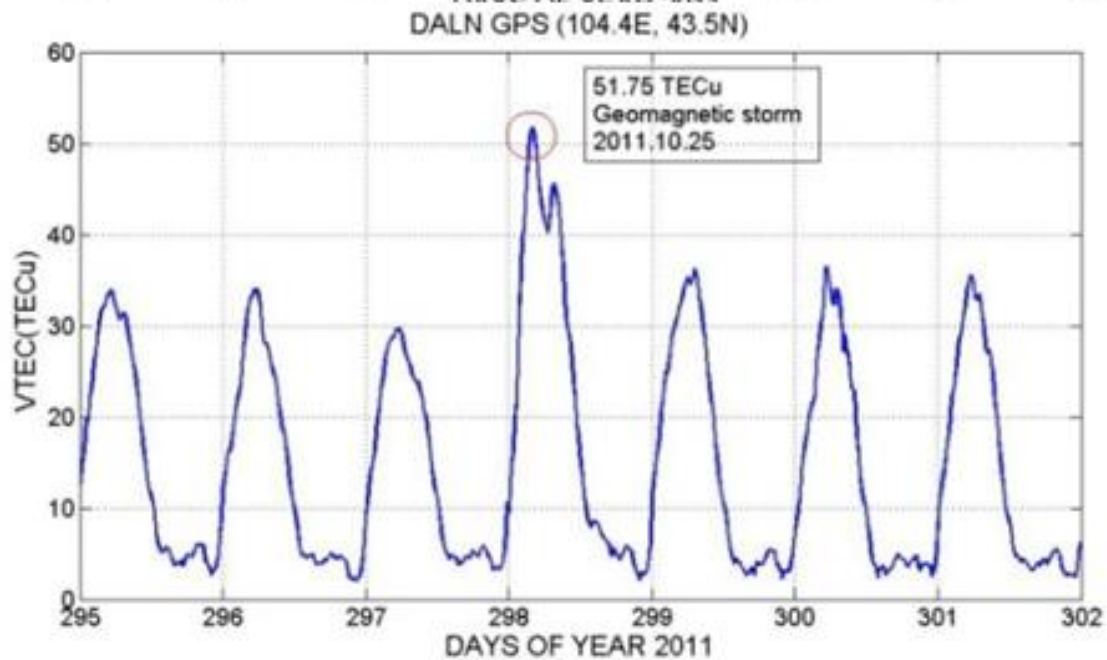
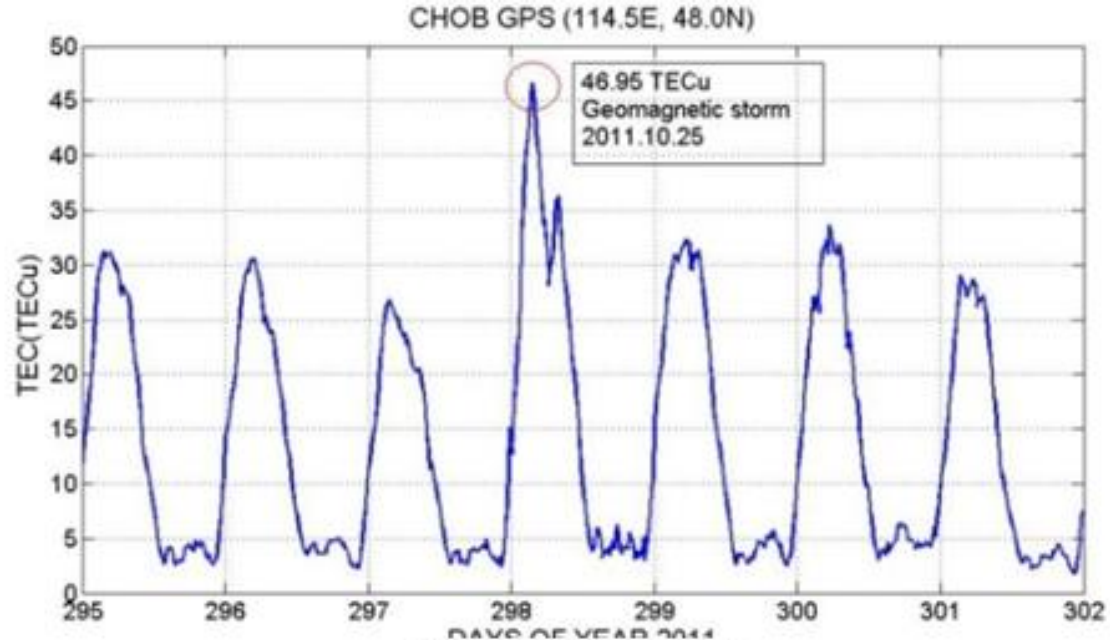


- St. Patrick's day – 17 March 2015 originated from Solar storm of 15 March 2015 at 2:10 UTC a partial halo coronal mass ejection (CME)
- Flare C9.1
- Series of radio bursts type of II/IV
- Dst = -223nT
- Doy 76 -17March increase 35-40TECU
- Doy 77 -18March decrease 10-20 TECU

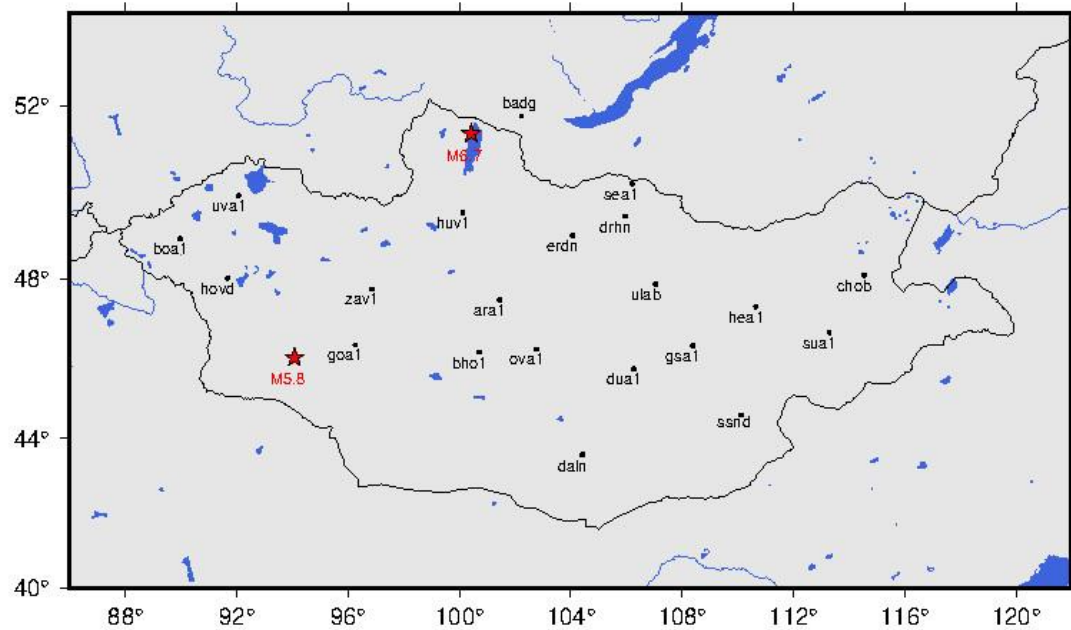


Geomagnetic activities

- Solar disturbances solar flares, CME
- 25 October 2011



Seismo-ionospheric anomalies



Two moderate to large EQ

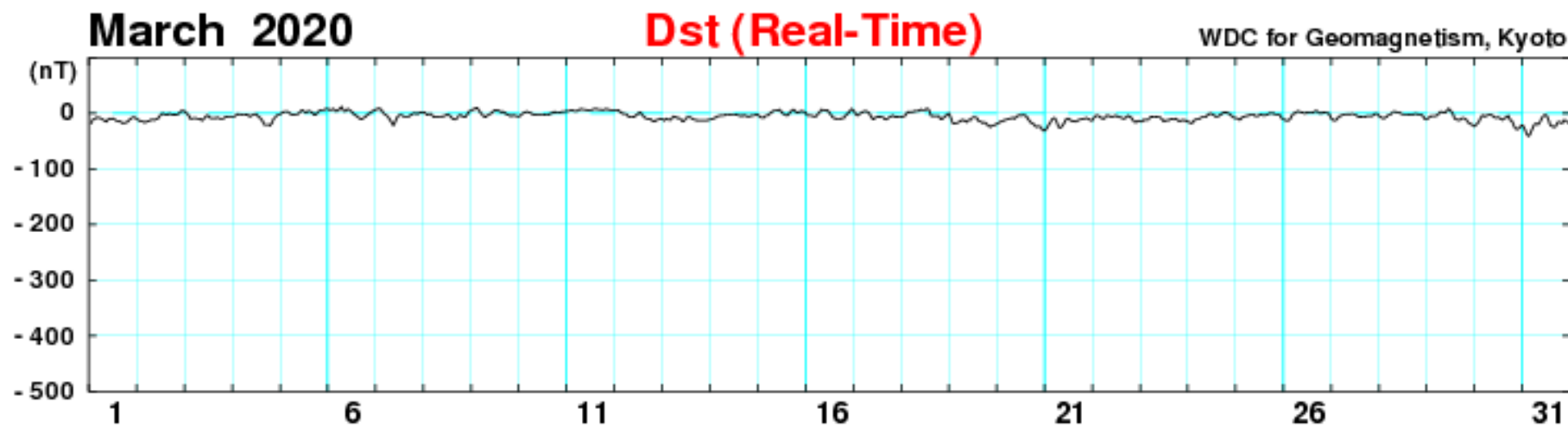
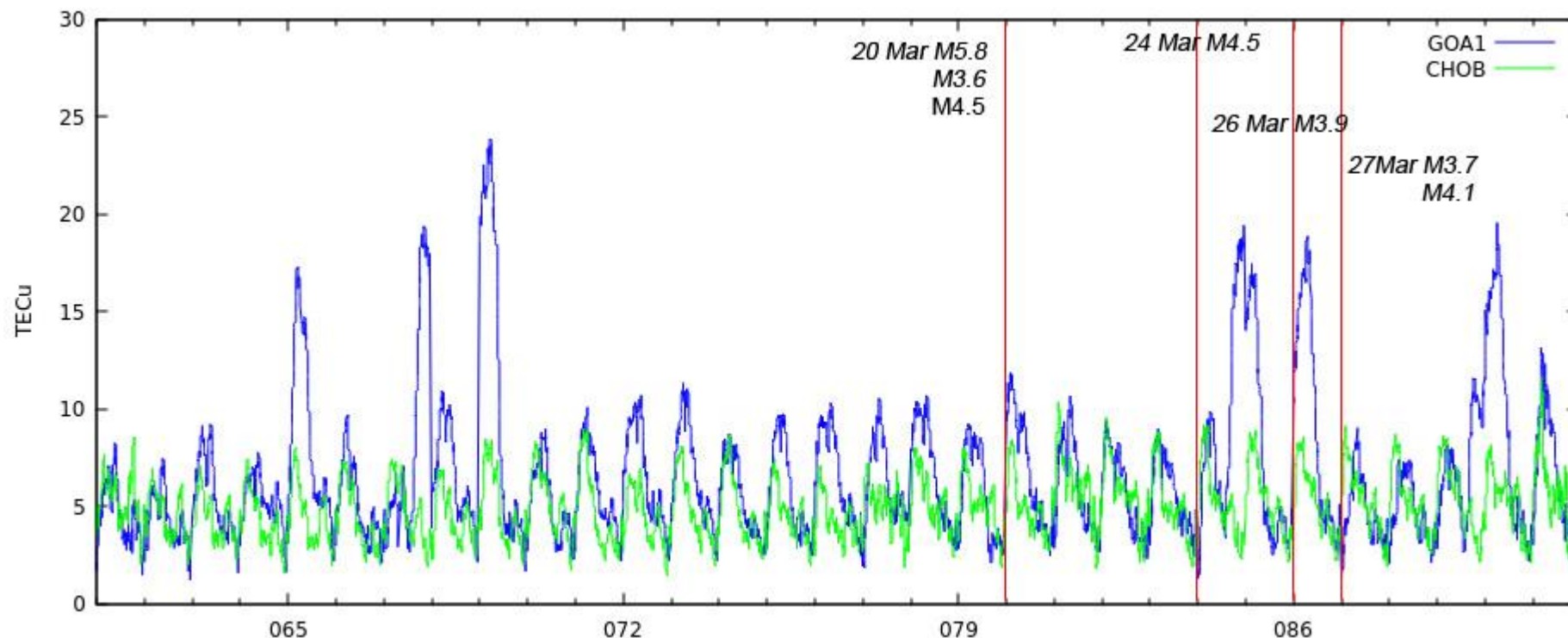
1. M5.8 Gobi Altay
2. M6.7 Hubsugul EQ

No	Location	Lon/Lat	Date	Magnitude, M	Depth, km	GPS station	ρ , km
1	Gobi-Altay	94.07E/46.06 N	20/03/2020	5.8	10	GOA1	312
2	Hubsugul	100.42E/51.38N 97.36E/52.34N	12/01/2021 21/02/2021	6.7 5.1	10 15.1	HUV1	760

- The radius of preparation zone is calculated (Dobrovolsky et al, 1979)
- $\rho = 10^{0.43M}$ km
- ρ – radius of preparation zone, M is earthquake magnitude

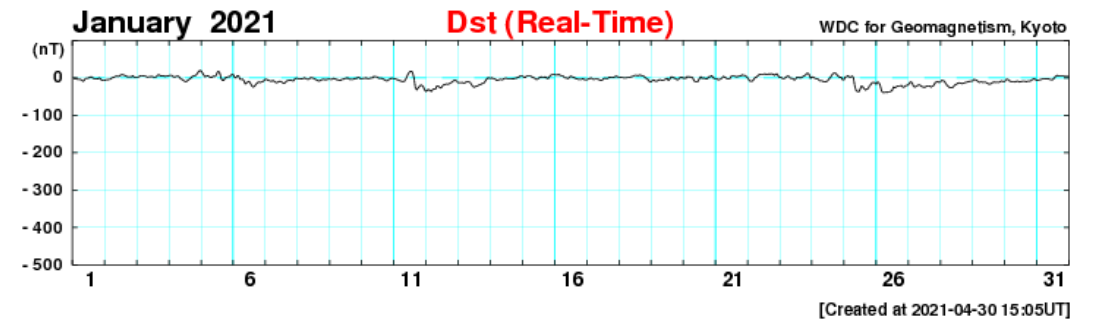
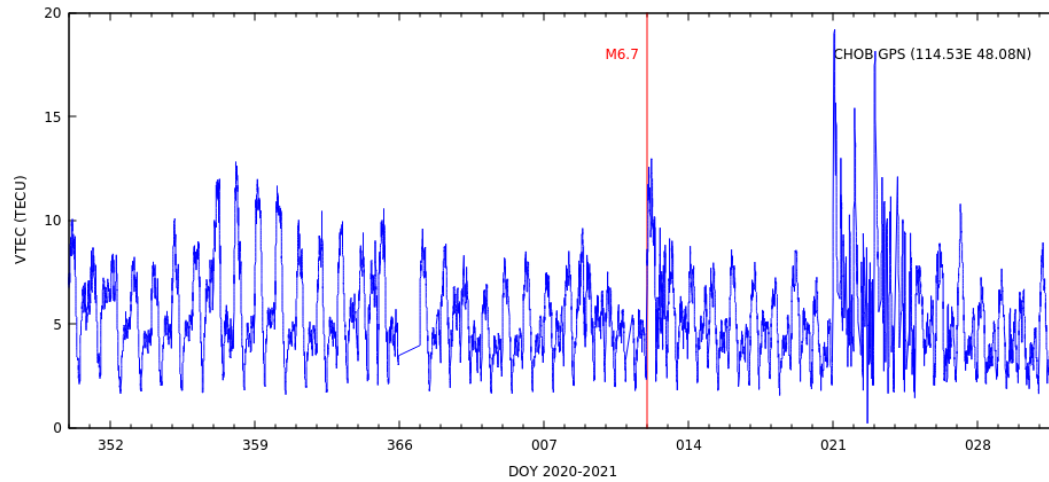
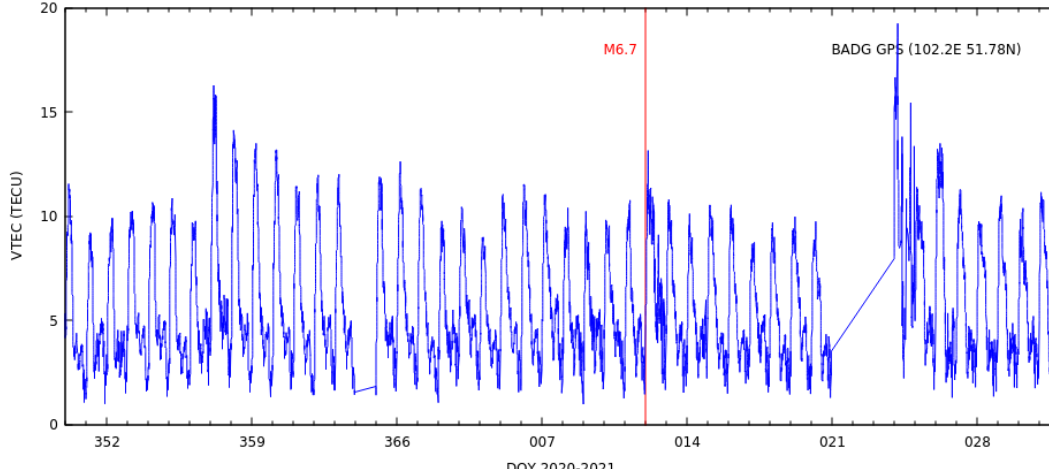
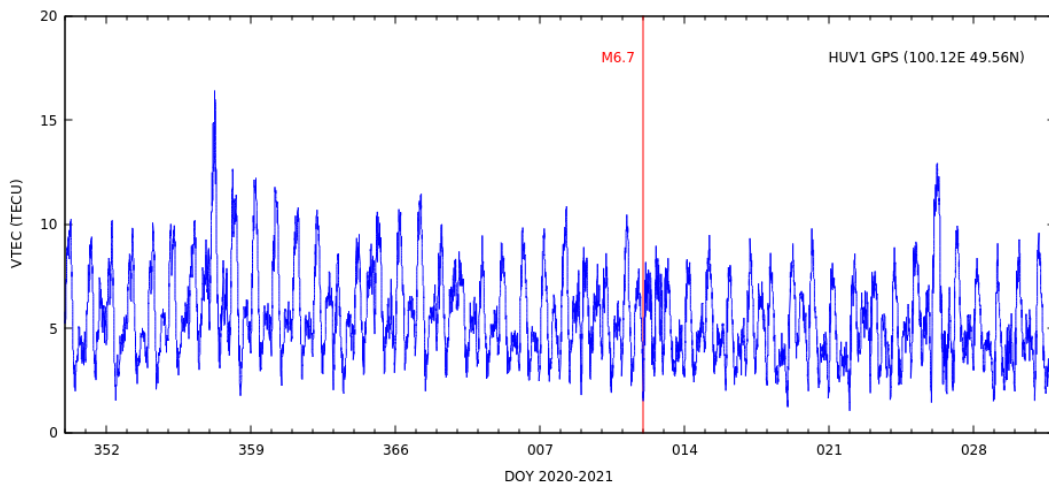
M5.8 Gobi-Altai EQ, 20/03/2020

- 20/03/2020
 - 1M5.8
 - 11:14LT M3.6
 - 11:56LT M4.5
- 24/03/2020
 - M4.5
- 26/03/2020
 - M3.9
- 27/03/2020
 - M3.7, M4.1
- 02/04/2020
 - M3.9



M6.7 Hubsugul 12/01/2021

- BADG IGS, HUV1, CHOB
- TEC enhancement prior to EQ on DOY 357



Summary

- Patterns of Ionosphere regular and irregular variations over Mongolia are presented in terms of the Total Electron Content derived from CGPS
- ionosphere over Mongolia has a general characteristics of mid-latitude ionosphere
- Solar and magnetic activities, and seismo-induced disturbances can also be detected